Optics Communications 284 (2011) 2613–2616

Contents lists available at ScienceDirect

Optics Communications

journal homepage: www.elsevier.com/locate/optcom

Discussion

Multi-channel plasmonic waveguide filters with disk-shaped nanocavities

Hua Lu, Xueming Liu *, Yongkang Gong, Leiran Wang, Dong Mao

State Key Laboratory of Transient Optics and Photonics, Xi'an Institute of Optics and Precision Mechanics, Chinese Academy of Sciences, Xi'an 710119, China

ARTICLE INFO

Article history:
Received 18 October 2010
Accepted 17 January 2011
Available online 1 February 2011

Keywords:
Surface plasmon polaritons
Integrated optics devices
Wavelength filtering devices

ABSTRACT

A kind of multi-channel plasmonic filters based on metal–insulator–metal waveguides with disk-shaped nanocavities is proposed and numerically investigated. By calculating the resonant mode of disk-shaped nanocavity, it is found that the radius and refractive index of the nanocavity effectively control the resonance wavelength, which is consistent with the results obtained by finite-difference time-domain method. The characteristics of resonance spectra are influenced by the gap width between the cavity and waveguide, as can be exactly analyzed by temporal coupled mode theory. In addition, multi-channel plasmonic filters are achieved by increasing the number of nanocavity.

1. Introduction

Electromagnetic waves trapped on metal-dielectric interfaces and coupled to propagating free electron oscillations in the metals, known as surface plasmon polaritons (SPPs), are regarded as the most potential way for the realization of highly integrated optical circuits because they significantly overcome the classical diffraction limit and can manipulate light in a nanoscale domain [1–3]. A number of devices based on SPPs, such as Mach–Zehnder interferometers [2,4], all-optical switches [5,6], splitters [2,7,8], modulators [9], beam manipulator [10,11], multiplexing sensor [12], polarization analyzer [13], optical amplifier [14], optical buffers [15], and Bragg reflectors [16] have been simulated numerically and demonstrated experimentally. Bragg reflectors, fabricated by periodically stacking two kinds of insulators/alternately modulating slit widths in metal–insulator–metal (MIM) [16,17]/insulator–metal–insulator (IMI) plasmonic waveguides [18], can achieve the wavelength-filtering function. The IMI waveguide exhibits less loss, but fails to confine light into a subwavelength scale and, thus, is not suitable for high optical integration [18]. The MIM waveguide exhibits strong light confinement and acceptable length for SPP propagation [16]. To overcome the complexity of fabrication and decrease the length for plasmonic Bragg structures, some simple plasmonic waveguide filters have been proposed, such as tooth-shaped filters [19], plasmonic filters with disk/ring resonators [2,20–22], and filters with rectangular resonators [23]. As key factors in these filters, optical resonators will be principal consistent elements of future plasmonic filters due to their simplicity, symmetry, and ease of fabrication [24]. The optical spectra of the designed structures mentioned above have one channel and, thus, can only filter single wavelength in communication. In order to design plasmonic filters with multiple channels, Zhou et al. proposed a quasiperiodic SPP bandgap structure to achieve plasmonic dual-channel filters [25]. Quite recently, a high-channel-count plasmonic filter with the MIM Fibonacci-sequence gratings is investigated [26]. Due to their complicated structures and long dimensions, these multi-channel plasmonic filters are not suitable for application in highly integrated optical circuits. Therefore, it is very meaningful to design simple and compact multi-channel plasmonic filters.

In this paper, a new kind of simple multi-channel plasmonic filters based on MIM waveguides with side coupled disk-shaped nanocavities is proposed and numerically investigated. By calculating the resonant mode of disk-shaped nanocavity, we find that the resonance wavelengths can be easily manipulated by adjusting the radius and refractive indices of the nanocavities, which is in good agreement with finite-difference time-domain (FDTD) simulations. The properties of resonance spectra are influenced by the gap width between the nanocavity and waveguide, which can be accurately analyzed by temporal coupled mode theory. The multi-channel filters may have important application on wavelength division multiplexing (WDM) systems in highly integrated optical circuits.

2. Model and simulations

The MIM plasmonic waveguide consists of two metallic claddings and a dielectric core with the width w_t, as shown in Fig. 1. When TM-polarized plane light wave is injected to the MIM structure, the incident light will be coupled into the waveguide and the SPP waves are formed on two metal interfaces. The width of dielectric core w_t is set to be 50 nm, which is similar to that of the waveguide in Ref. [19]. Here, we investigate the SPP characteristics in the MIM waveguide with a side coupled disk-shaped nanocavity. The other parameters are assumed as $r=100$ nm and $d_t=20$ nm. The insulator in the metal slit and cavity is air. The metal is assumed as silver, whose complex

* Corresponding author. Tel.: +86 2988881560; fax: +86 2988887603.
E-mail addresses: liuxueming72@yahoo.com, liuxm@opt.ac.cn (X. Liu).

0030-4018/$ – see front matter © 2011 Elsevier B.V. All rights reserved.
doi:10.1016/j.optcom.2011.01.046

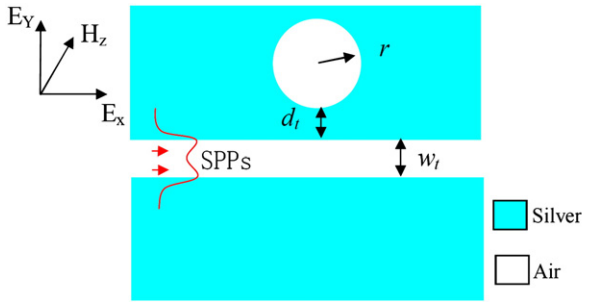

Fig. 1. Schematic diagram of plasmonic waveguide. r: radius of nanocavity, w_t: metal slit width, and d_t: gap width between the cavity and waveguide.

relative permittivity can be characterized by the well-known Drude model

$$\varepsilon_m(\omega) = \varepsilon_\infty - \frac{\omega_p^2}{\omega(\omega + i\gamma)} \tag{1}$$

where ε_∞ is the dielectric constant at the infinite frequency, γ and ω_p represent the electron collision frequency and bulk plasma frequency, respectively. ω is the angular frequency of incident light. These parameters for silver can be set as $\varepsilon_\infty = 3.7$, $\omega_p = 9.1$ eV, and $\gamma = 0.018$ eV [17]. To study the transmission characteristics, the incident wave is propagated from the left to the right side of the waveguide. P_{in} and P_{out} present the power at incident and transmitted ports, respectively. The disk-shaped nanocavity is 500 nm away from the input and output ports. The transmission is defined as $T = P_{out}/P_{in}$ [19]. The properties of SPP propagation are investigated by the FDTD method. In FDTD simulations, the spatial steps are set as $\Delta x = 5$ nm and $\Delta y = 5$ nm. The temporal step is $\Delta t = \Delta x/2c$. Fig. 2(a) shows that the transmission spectrum of our waveguide has a dip at the wavelength of 490 nm, which is a typical characteristic of filter. The field distributions in Fig. 2(b) and (c) reveal that the incident lights are completely reflected and partly pass through the waveguide with incident wavelengths of 490 and 510 nm, respectively. The results are consistent with the transmission spectrum in Fig. 2(a).

As shown in Fig. 2(b), the disk-shaped nanocavity functions as a disk resonator. The standing wave modes in the air disk resonator will be excited [22], and the characteristic equation can be derived from [27] and is given by

$$k_d \frac{H_n^{(1)'}(k_m r)}{H_n^{(1)}(k_m r)} = k_m \frac{J_n'(k_d r)}{J_n(k_d r)}, \tag{2}$$

where $k_{d/m} = k(\varepsilon_{d/m})^{1/2}$ represents the wave vectors in the dielectric cavity/metal, and k is the wave number. r is the radius of nanocavity. ε_d and ε_m are the relative permittivities of dielectric and metal, respectively. J_n and J'_n stand for the first kind Bessel function with the order n and its derivation, and $H_n^{(1)}$ and $H_n^{(1)'}$ are the first kind Hankel function with the order n and its derivation, respectively. The fundamental mode, corresponding to the first-order Bessel and Hankel functions, is taken into account. From Eq. (2), we can see that the resonant mode is controlled by r and n_t (i.e., $(\varepsilon_d)^{1/2}$). The transmission spectrum near the resonant mode can be described by the temporal coupled mode theory [28,29], and the transmission T is described as

$$T(\omega) = \frac{(\omega - \omega_0)^2 + (1/\tau_i)^2}{(\omega - \omega_0)^2 + (1/\tau_i + 1/\tau_\omega)^2}, \tag{3}$$

where ω is the frequency of incident light and ω_0 presents the resonance frequency. $1/\tau_i$ is the decay rate of the field induced by the internal loss in the nanocavity, and $1/\tau_\omega$ stands for the decay rate by

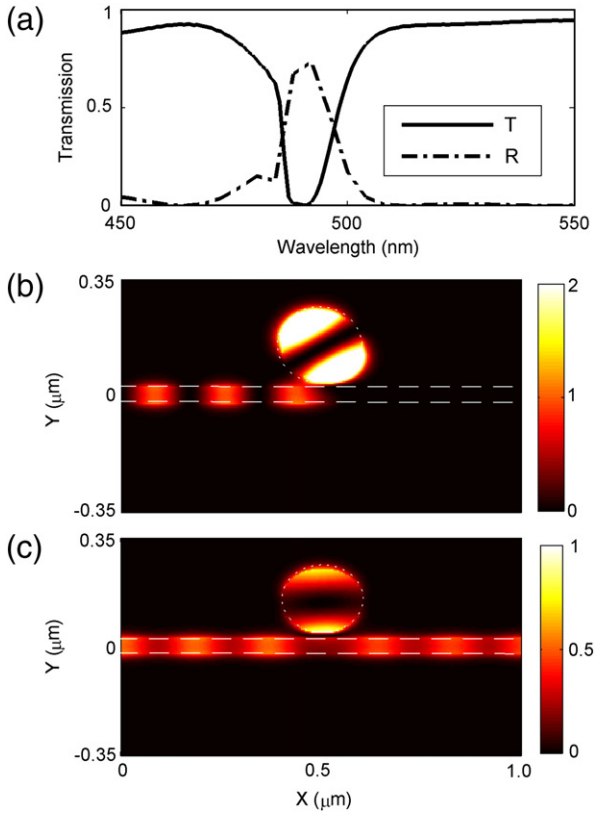

Fig. 2. (a) Transmission and reflection spectra of the filter with a side coupled disk-shaped nanocavity. (b)–(c): The average field distributions of $|H_z|^2$ with incident wavelengths of 490 and 510 nm. The color scale is saturated in (b).

the power escape through the waveguide. At the resonance frequency ω_0, the transmission spectrum has a dip with a minimal value of $(1/\tau_i)^2/(1/\tau_\omega + 1/\tau_i)^2$, as shown in Fig. 2.

The resonance wavelength as a function of the radius and refractive index of nanocavity is investigated by the characteristic equation of resonant mode of the disk-shaped nanocavity and the FDTD method. The red-shift of resonance wavelength changes almost linearly with the radius (r) of cavity, as shown in Fig. 3(a). The relation between the resonance wavelength and refractive index (n_t) is depicted in Fig. 3(b). It is found that the red-shift of resonance wavelength approximately presents linear relation with n_t. The results obtained by solving Eq. (2). In FDTD simulations, the transmitted-dip wavelengths are obtained at different parameters (i.e., the radius and refractive index of nanocavity). In Fig. 3, we can find that the wavelengths are in accordance with the theoretic results.

Another structure parameter d_t, which represents the coupling distance between the nanocavity and waveguide, is an important factor influencing the resonance spectrum. The influence of d_t on the resonance spectrum is investigated by FDTD simulations. As can be seen in Fig. 4, the bandwidth of the resonance spectrum decreases and the minimum (T_{min}) of transmission dip increases for increasing d_t, which can be explained by temporal coupled mode theory. The increase of d_t results in weaker coupling and smaller $1/\tau_\omega$ [30]. The variation of $1/\tau_i$ can be neglected when only d_t is altered. Thus $T_{min} = (1/\tau_i)^2/(1/\tau_\omega + 1/\tau_i)^2$ increases as $1/\tau_\omega$ decreases. Full width at half maximum of the reflection spectrum around the resonance wavelength is $\Delta_{FWHM} \approx 4\pi c(1/\tau_\omega + 1/\tau_i)/\omega_0^2$, as can be derived from Ref. [28]. The resonance spectral width exhibits the same variation as Δ_{FWHM} which decreases when $1/\tau_\omega$ decreases. The resonance spectrum has a slight blue-shift, which is consistent with the results in Refs. [23,30]. Normally, transmission spectrum around the resonance wavelength exhibits Lorentzian profile, which can be

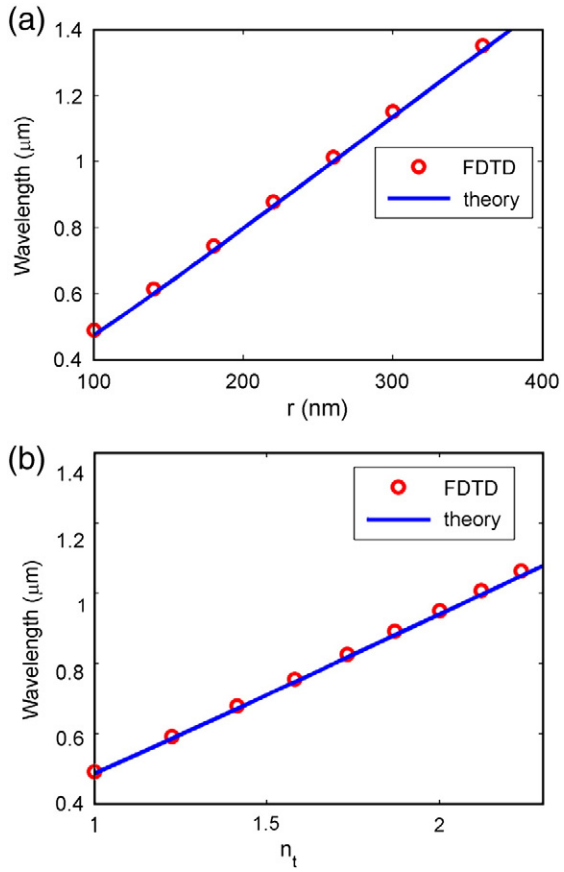

Fig. 3. (a) Relationship between the resonance wavelength and r with $n_t = 1$. (b) Relationship between the resonance wavelength and n_t with $r = 100$ nm.

derived from Eq. (3). The shape of the transmission spectrum is asymmetric due to the dispersion and loss of MIM waveguide [30], as shown in Fig. 4.

3. Design of multi-channel plasmonic filters

Dual-channel filters can be formed by integrating two side coupled nanocavities into a MIM plasmonic waveguide. Fig. 5(a) and (b) show the transmission spectra of dual-channel filters with two nanocavities in a metallic cladding and in two different metallic claddings, respectively. The filtering wavelengths can be manipulated by adjusting the radius of nanocavity in the two kinds of plasmonic filters. Meanwhile, there exist the same filtering wavelengths for the

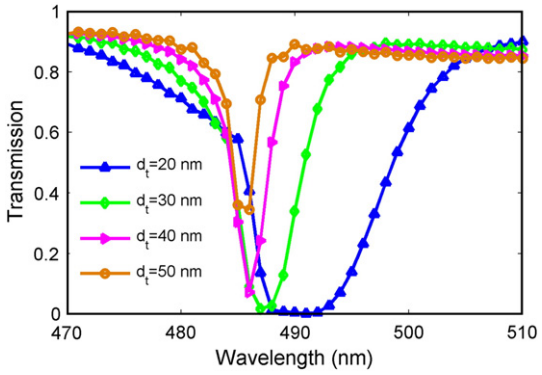

Fig. 4. Transmission spectra with different d_t.

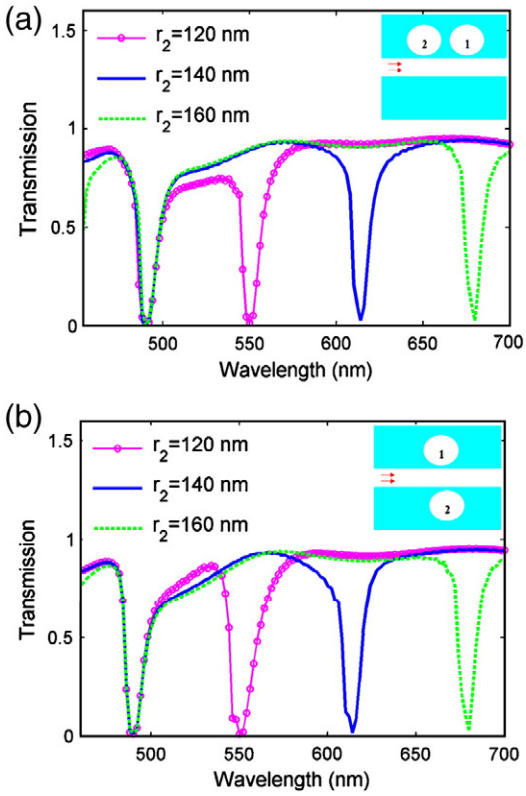

Fig. 5. Transmission spectra with different r_2 with two cavities in (a) a metallic cladding and (b) different metallic claddings.

two dual-channel filters with identical radii. Therefore, dual-channel filters can be obtained by the above two manners of integration.

The amount of filtering channel is effectively controlled by adjusting the number of nanocavity near the waveguide. Here, a four-channel filter is designed to study the characteristic of SPP propagation. The radii of four side coupled disk-shaped nanocavities introduced in the MIM plasmonic waveguide are assumed as $r_1 = 110$ nm, $r_2 = 125$ nm, $r_3 = 140$ nm, and $r_4 = 155$ nm. The transmission spectrum and the average field distributions of $|H_z|^2$ with filtering wavelengths are simulated by the FDTD method. The filtering wavelengths are 518, 568, 615, and 662 nm, as shown in Fig. 6(a). The field distributions show that the incident lights with these wavelengths are reflected completely, as well as excite resonant modes in corresponding nanocavities, as can be seen in Fig. 6(b)–(e).

4. Conclusions

In this paper, based on MIM plasmonic waveguides with side coupled disk-shaped nanocavities, a new kind of simple multi-channel filters has been numerically investigated. By calculating the resonant mode of the disk-shaped nanocavity, we find that the resonant wavelengths can be easily manipulated by adjusting the radius and refractive index of the nanocavity, which is coincident with FDTD results. The bandwidth and minimal value of resonance spectra are affected by the gap width between the nanocavity and waveguide, which can be accurately analyzed by temporal coupled mode theory. In addition, the amount of filtering channel can be effectively controlled by adjusting the number of nanocavity. Two types of dual-channel filters and a four-channel filter are designed to study the characteristics of SPP propagation. The proposed multi-channel filters have important potential applications on WDM systems in highly integrated optical circuits due to their simplicity and compact size.

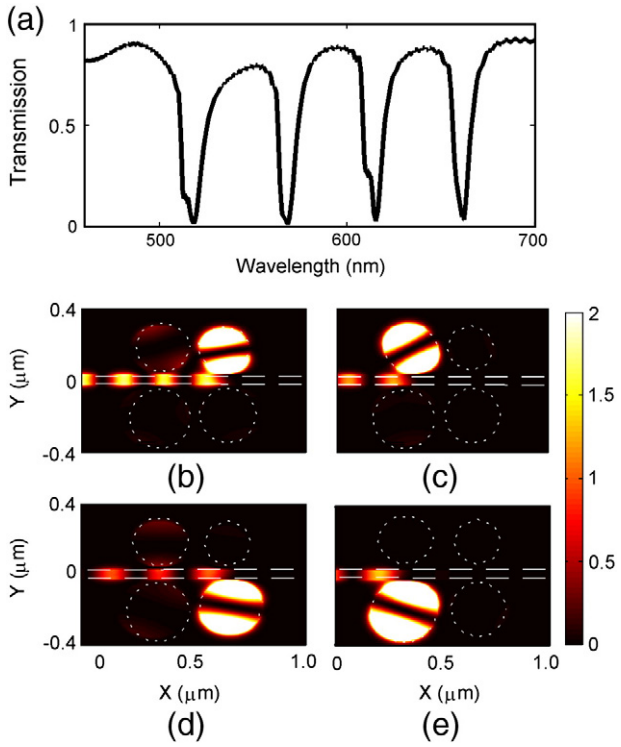

Fig. 6. (a) Transmission spectrum of the MIM waveguide with four side coupled disk-shaped nanocavities. (b)–(e): Field distributions of $|H_z|^2$ at filtering wavelengths of 518, 568, 615, and 662 nm.

Acknowledgements

This work was supported by the National Natural Science Foundation of China under Grant 10874239 and 10604066.

References

[1] W.L. Barnes, A. Dereux, T.W. Ebbesen, Nature 424 (2003) 824.
[2] S.I. Bozhevolnyi, V.S. Volkov, E. Devaux, J.Y. Laluet, T.W. Ebbesen, Nature 440 (2006) 508.
[3] C. Genet, T.W. Ebbesen, Nature 445 (2007) 39.
[4] B. Wang, G.P. Wang, Opt. Lett. 29 (2004) 1992.
[5] G.A. Wurtz, R. Pollard, A.V. Zayats, Phys. Rev. Lett. 97 (2006) 057402.
[6] W. Zhang, S. Yu, Opt. Commun. 283 (2010) 2622.
[7] G. Veronis, S. Fan, Appl. Phys. Lett. 87 (2005) 131102.
[8] M. He, J. Liu, Z. Gong, Y. Luo, X. Chen, W. Lu, Opt. Commun. 283 (2010) 1784.
[9] T. Nikolajsen, K. Leosson, S.I. Bozhevolnyi, Appl. Phys. Lett. 85 (2004) 5833.
[10] H. Kim, J. Park, B. Lee, Opt. Lett. 34 (2009) 2569.
[11] L.L. Yin, V.K. Vlasko-Vlasov, J. Pearson, J.M. Hiller, J. Hua, U. Welp, D.E. Brown, C.W. Kimball, Nano Lett. 5 (2005) 1399.
[12] D.V. Oosten, M. Spasenovic, L. Kuipers, Nano Lett. 10 (2010) 286.
[13] S.Y. Yang, W.B. Chen, R.L. Nelson, Q.W. Zhan, Lett 34 (2009) 3047.
[14] I.D. Leon, P. Berini, Nat. Photonics. 4 (2010) 382.
[15] Q.Q. Gan, Y.J.J. Ding, F.J. Bartoli, Phys. Rev. Lett. 102 (2009) 056801.
[16] B. Wang, G.P. Wang, Appl. Phys. Lett. 87 (2005) 013107.
[17] Z.H. Han, E. Forsberg, S. He, IEEE Photonics. Technol. Lett. 19 (2007) 91.
[18] J.W. Mu, W.P. Huang, J. Lightwave. Technol. 27 (2009) 436.
[19] X.S. Lin, X.G. Huang, Opt. Lett. 33 (2008) 2874.
[20] H. Lu, X. Liu, D. Mao, L. Wang, Y. Gong, Opt. Express 18 (2010) 17922.
[21] X. Wang, P. Wang, C. Chen, J. Chen, Y. Lu, H. Ming, Q. Zhan, J. Appl. Phys. 107 (2010) 124517.
[22] S.S. Xiao, L. Liu, M. Qiu, Opt. Express 14 (2006) 2932.
[23] A. Noual, Y. Pennec, A. Akjouj, B. Djafari-Rouhani, L. Dobrzynski, J. Phys. Condens. Matter 21 (2009) 375301.
[24] I. Chremmos, J. Opt. Soc. Am. A 26 (2009) 2623.
[25] L. Zhou, X. Yu, Y. Zhu, Appl. Phys. Lett. 89 (2006) 051901.
[26] Y. Gong, X. Liu, L. Wang, Opt. Lett. 35 (2010) 285.
[27] S.L. Qiu, Y.P. Li, J. Opt. Soc. Am. B 26 (2009) 1664.
[28] Q. Li, T. Wang, Y.K. Su, M. Yan, M. Qiu, Opt. Express 18 (2010) 8367.
[29] Z. Yu, G. Veronis, S. Fan, Appl. Phys. Lett. 92 (2008) 041117.
[30] Z.J. Zhong, Y. Xu, S. Lan, Q.F. Dai, L.J. Wu, Opt. Express 18 (2010) 79.